Using the TOPS-MODE approach to fit multi-target QSAR models for tyrosine kinases inhibitors

8 AUTHORS, INCLUDING:

Giovanni Marzaro
University of Padova
30 PUBLICATIONS   259 CITATIONS

SEE PROFILE

Adriana Chilin
University of Padova
89 PUBLICATIONS   764 CITATIONS

SEE PROFILE

Eugenio Uriarte
University of Santiago de Compostela
358 PUBLICATIONS   6,941 CITATIONS

SEE PROFILE

Ignazio Castagliuolo
University of Padova
110 PUBLICATIONS   2,458 CITATIONS

SEE PROFILE

Original article

Using the TOPS-MODE approach to fit multi-target QSAR models for tyrosine kinases inhibitors

Giovanni Marzaro [a,b,*], Adriana Chilin [a], Adriano Guiotto [a], Eugenio Uriarte [b], Paola Brun [c], Ignazio Castagliuolo [c], Francesca Tonus [a], Humberto González-Díaz [b,d]

[a] Department of Pharmaceutical Sciences, University of Padova, via marzolo 5, 35131 Padua, Italy
[b] Unit of Bioinformatics & Connectivity Analysis (UBICA), Institute of Industrial Pharmacy, Faculty of Pharmacy, Department of Organic Chemistry, University of Santiago de Compostela, 15782, Spain
[c] Department of Histology, Microbiology and Medical Biotechnology, University of Padova, 35131, Italy
[d] Department of Microbiology and Parasitology, University of Santiago de Compostela, 15782, Spain

ABSTRACT

Tyrosine kinases constitute an eligible class of target for novel drug discovery. They resulted often overexpressed and/or deregulated in several cancer diseases. Thus, the development of novel tyrosine kinases inhibitors is of value, as well as the finding of novel cheminformatic tools for their design. Among the different ways to rationally design novel compounds, the Quantitative Structure-Activity Relationship (QSAR) plays a key role. The QSAR approach, in fact, allow the prediction of activity against a number of targets (multi-target QSAR), thus leading to models able to predict not only the activity of a compound, but also its selectivity versus a set of targets. Despite it is well known that tyrosine kinase inhibitors have to show multi-kinases inhibitory potency to be useful in anticancer therapy, only few multi-target computational tools have been developed to help medicinal chemists in the design of novel compounds. Herein we present the development of several multi-target classification QSAR (mtc-QSAR) models useful to assess the activity profile of the tyrosine kinases inhibitors.

© 2011 Elsevier Masson SAS. All rights reserved.

1. Introduction

The scientific interest in tyrosine kinases (TKs) as drug targets has been rapidly increased in the last years. TKs are key regulatory protein of the cell cycle progression as they are involved in most signaling pathways. Overexpression or disregulation of TKs activity has been associated with cancer, inflammation, diabetes and other diseases [1,2]. Several strategies to inhibit TKs activity have been developed, including the use of small molecule ATP-mimics (TKs inhibitors, TKIs) [3]. Unlike other inhibitor tools (such as monoclonal antibodies or nonsense nucleotides), several TKIs showed a broad spectrum of activity, i.e. some of them are able to efficiently inhibit more than one TK [4]. This feature is very useful to reduce the drug resistance phenomena onset as recently reported [5]. Despite the relevance of these last observations and even if a number of TKs have been proved to be involved in cancer diseases, majority of TKIs has been designed to be selective only against a single TK or, at most, they have been assayed only versus a close panel of TKs.

TKIs represent also a promising class for the development of antiparasite drugs. The effects of seven TKIs (staurosporine, genistein, methyl 2,5-dihydroxycinnamate, tyrphostins B44 and B46, lavendustin A and R03) on the erythrocytic cycle of the malaria parasite *Plasmodium falciparum* have been examined. Recently, antiparasite activities of 52 EGFR TKIs analogs of isoflavone were measured against *Sarcocystis neurona*, *Neospora caninum*, and *Cryptosporidium parvum* grown in BM and HCT-8 cell cultures [6,7].

Because of the high importance of TKIs in pharmaceutical area, the development of methods for efficient identification of novel drug candidates has therefore received high attention. Several docking [8,9] and QSAR [10–12] studies appeared in the literature, but only few works focused on the multi-target aspect of TKIs [13].

2. Material and methods

2.1. Chemistry

Compounds used for the validation of the QSAR models were synthesized as previously described [14].

Table 1
List of descriptors employed.

Descriptor symbol	Type of descriptor
$^{\lambda}\mu$	Distance
$^{d}\mu$	Dipole moment
$^{h}\mu$	Hydrophobicity
$^{r}\mu$	Molar refractivity
$^{ps}\mu$	Polar surface
$^{p}\mu$	Polarizability
$^{vdw}\mu$	Van der Waals volume
$^{gm}\mu$	Gasteiger-Marsilii partial charge
$^{m}\mu$	Atomic mass

Table 2
Dipole moment values at different calculation steps for three example molecules.

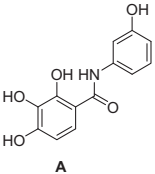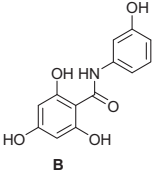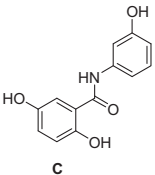| Compound	$^{d}\mu_1$	$^{d}\mu_2$	$^{d}\mu_3$	$^{d}\mu_4$	$^{d}\mu_5$
A	7.79	66.36	116.06	496.79	1392.78
B	7.79	66.36	116.06	500.79	1419.93
C	6.93	61.62	104.26	455.45	1264.10

2.2. In vitro kinase assays

Activated tyrosine kinases (abl, src, EGFR, FGFR1, KDR and PDGFRβ) were purchased from Sigma Aldrich or Calbiochem and were diluted in kinase dilution buffer (5 mM MOPS pH 7.2, 2.5 mM glycerol 2-phosphate, 5 mM MgCl$_2$, 0.4 mM EGTA, 0.4 mM EDTA, 0.05 mM DTT, 0.5 mM BSA). Reactions were set up in pre-cooled microcentrifuge tubes. Tested compounds have been added with: active kinase at final concentration of 200 ng/ml; 0.2 mg/ml substrate solution (Myelin Basic Protein, Sigma); 0.05 mM ATP and 0.25 μCi of [γ-^{32}P]ATP (PerkinElmer, Monza, MI) to a final reaction volume of 25 μl. The final concentration of tested compounds was 0.1 μM. Negative controls were prepared replacing the substrate solution with water whereas positive controls were set up replacing test molecules with water. Reactions were carried out at 30 °C for 20 min and finally stopped by the addition of loading buffer containing 0.25 mM β-mercaptoethanol. Samples were then subjected to electrophoresis on 10% w/v SDS-PAGE gel. Gels were dried, and phosphorylated myelin basic protein was identified by autoradiography. The VersaDoc Quantity One software (BioRad) was used for densitometric analysis.

2.3. Dataset for mtc-QSAR models generation

Structure and biological data for 1300 compounds were retrieved from literature (see Supporting Information for bibliography). Compounds tested against a set of 8 TKs constituted by 3 cytoplasmic TKs (abl, lck and src) and 5 receptor TKs (EGFR, FGFR1, KDR, PDGFRβ and VEGFR-1) where chosen. Only the data regarding TKs cells free assays were taken in consideration and only if the assays were performed measuring the inhibition of a poly-Tyr synthetic peptide phosphorylation (i.e. no autophosphorylation assays were considered). Both reversible and irreversible TKIs were considered. pIC$_{50}$ values were converted to the corresponding IC$_{50}$ values. 2D structure of each compound was converted to the SMILES notation using ChemAxon software [15]. Because of several

compounds were tested against more than one TKs, the total amount of cases in the dataset was 1771. The overall dataset have been randomly split into a training set and an internal validation set, using a 3:1 splitting ratio. The internal validation set has been used for a first validation of the models after their generation.

2.4. Dataset for mtc-QSAR models evaluation

Structure and biological data for 13 compounds assayed versus 7 of the 8 TKs considered were retrieved from literature. 2D structure of each compound was converted to the SMILES notation using ChemAxon software.

2.5. mtc-QSAR models generation

The dataset used to derive and to validate the QSAR models has been prepared as follow. To each m cases (m = 1771) a classifying dependent variable (Class, C) was assessed, being C = 1 if the compound was active with an IC$_{50}$ lower than an established cut-off of activity, and C = 0 if higher. Variable C was used as input to codify the activities. Five cut-off of activity were used (respectively 0.05, 0.1, 0.5, 1.0 and 5.0 μM), thus 5 mtc-QSAR models were finally derived.

Table 3
Dataset statistics.

TK	Number of cases	Active cases at 5.00 μM [%]	Active cases at 1.00 μM [%]	Active cases at 0.50 μM [%]	Active cases at 0.10 μM [%]	Active cases at 0.05 μM [%]
abl	102	35.3	24.5	23.5	18.6	12.7
lck	91	96.7	91.2	81.3	65.9	57.1
src	434	75.3	65.2	61.8	52.1	43.5
EGFR	457	75.7	66.1	63.9	54.9	47.0
FGFR-1	98	88.8	71.4	64.3	30.6	13.3
KDR	274	87.6	77.4	65.7	48.2	36.5
PDGFRβ	240	47.5	16.3	15.0	14.2	12.9
VEGFR-1	75	61.3	37.3	17.3	1.3	0.0
Total	1771	72.5	58.8	53.6	42.5	34.6

Then, starting from SMILES notation, for each *i* compound (*i* = 1300) the spectral moments $^{weight}\mu_{k,i}$ at *k* steps (*k* ranging from 1 to 5) of a set of molecular descriptors (*e.g.* $^{d}\mu_{k,i}$; see Table 1 for descriptors code explanation) were calculated employing the TOPS-MODE approach of the MODES-LAB software [16].

The TOPS-MODE approach has been widely described elsewhere [17–19], thus herein only a concise description will be presented. Briefly, in the TOPS-MODE (TOPological Substructure Molecular

DEsign) the spectral moments (*i.e.* the molecular descriptors) are calculated as the sum of the main diagonal entries of the bond adjacency matrix. In the matrix, the non-diagonal entries are ones or zeroes (thus indicating the presence or the absence of a bond between a pair of atoms), while the diagonal entries indicate the bond weights. Nine weights can be used in TOPS-MODE (see Table 1), and several algorithms for the weighting are applied, depending from the calculation step (*k*) employed [17–19]. The use
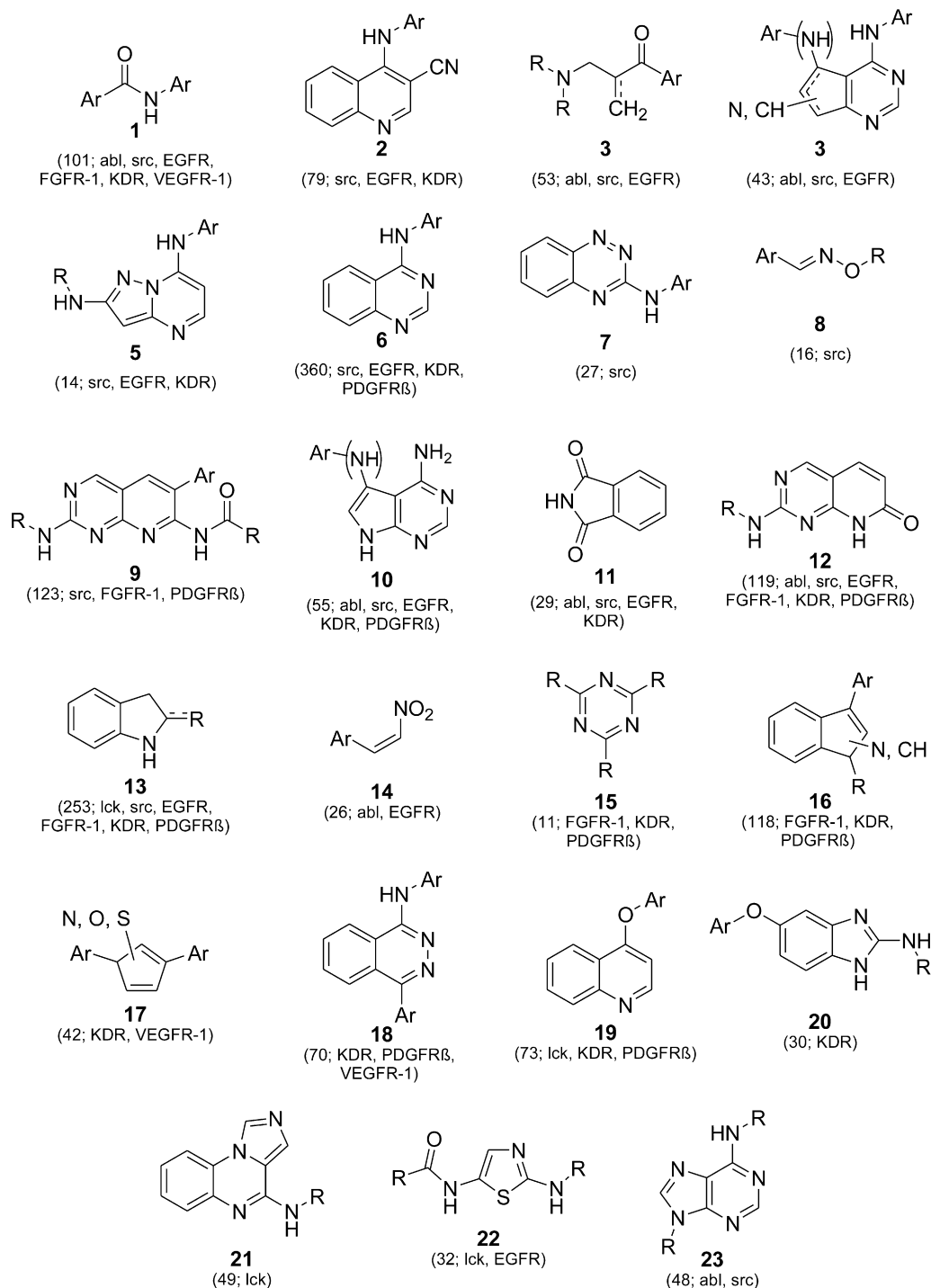

Fig. 1. List of the 23 scaffolds of the compounds in the dataset. Above each scaffold in brackets are reported the number of cases in the dataset and the TKs involved in biological evaluation).

Table 4
Summary of the mtc-QSAR models derived.

Cut-off [μM]	Set	Sensitivity [%]	Specificity [%]	Accuracy [%]	False positive[a]	False negative[b]	Variables entered	F-test value[c]	Chi-squared value
5.00	Train	80.87	80.48	80.59	188	70	8	84.45	572.98
	Validation	76.86	80.37	79.41	63	28			
	Total	**79.88**	**80.45**	**80.29**	**251**	**98**			
1.00	Train	83.55	84.14	83.90	124	90	8	166.36	908.21
	Validation	79.67	85.00	82.81	39	37			
	Total	**82.58**	**84.36**	**83.63**	**163**	**127**			
0.50	Train	83.44	83.17	83.30	120	102	8	171.59	947.17
	Validation	79.02	84.39	81.90	37	43			
	Total	**82.34**	**83.47**	**82.95**	**157**	**145**			
0.10	Train	83.90	84.25	84.05	89	123	8	165.65	917.94
	Validation	81.89	85.64	83.48	27	46			
	Total	**83.40**	**84.59**	**83.91**	**116**	**169**			
0.05	Train	82.51	82.61	82.54	80	152	8	122.44	734.37
	Validation	80.28	81.05	80.54	29	57			
	Total	**81.95**	**82.22**	**82.04**	**109**	**209**			

[a] Number of compounds inactive at the given cut-off but classified as active by the model.
[b] Number of compounds active at the given cut-off but classified as inactive.
[c] Test of significance of distances at $p < 0.00$.

of several calculation steps is of fundamental importance in order to obtain molecular descriptors able to highlight the small local differences between very similar molecules. As reported in the example in Table 2, at least four calculation steps are required to distinguish the dipole moment of two isomers (compare compounds A and B). On the contrary, for more different molecules just a single step could be sufficient (compare compounds A and C or B and C).
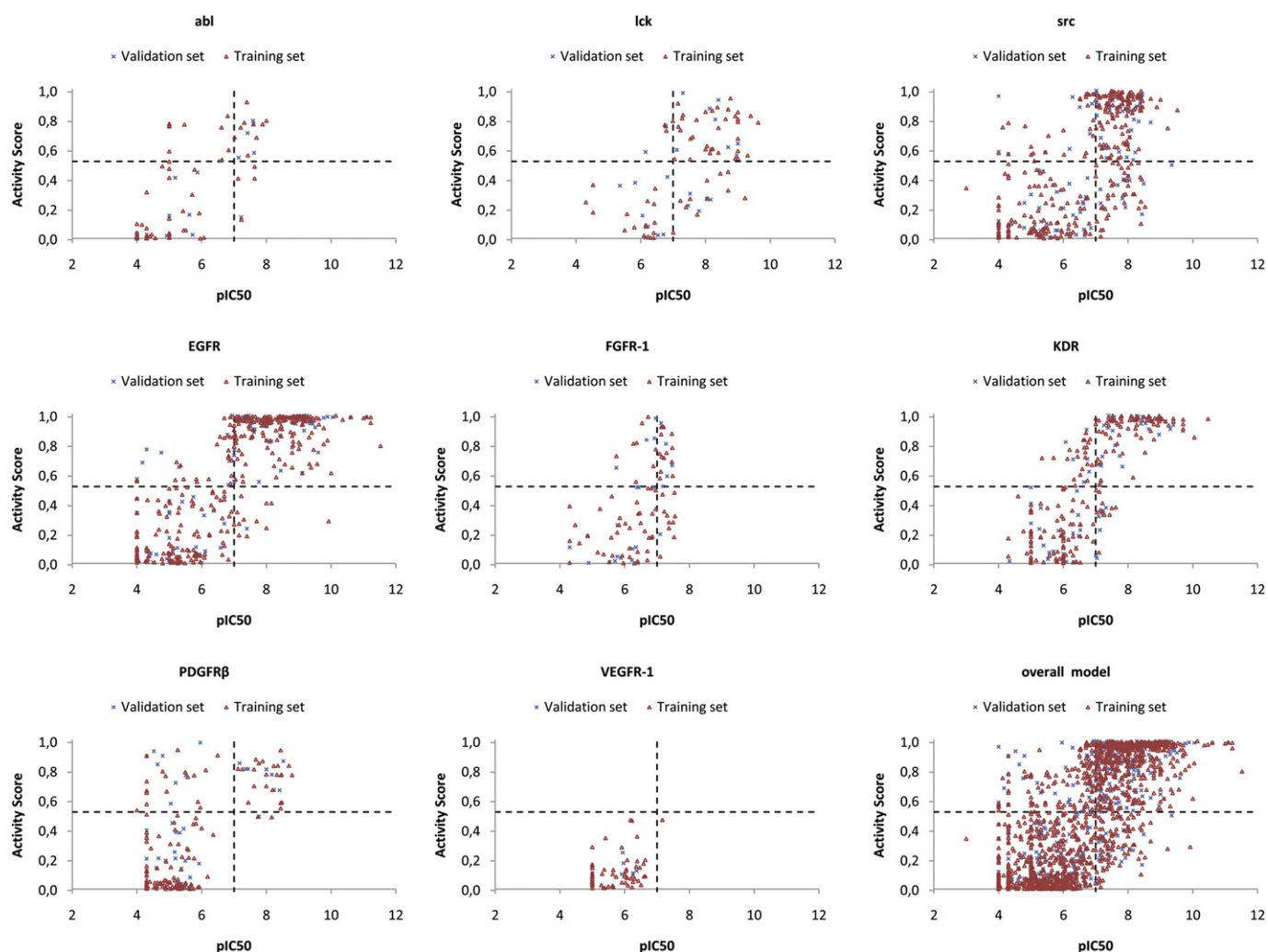

Fig. 2. Graphical representation of the mtc-QSAR model accuracies (cut-off = 0.1 μM). For each graphic: the upper left panel contains the false positive cases; the lower right panel contains the false negative cases; the upper right and the lower left panels contain the correctly predicted cases (active and inactive, respectively). The training set cases are depicted as red triangles, while the internal validation cases are depicted as cyan crosses.
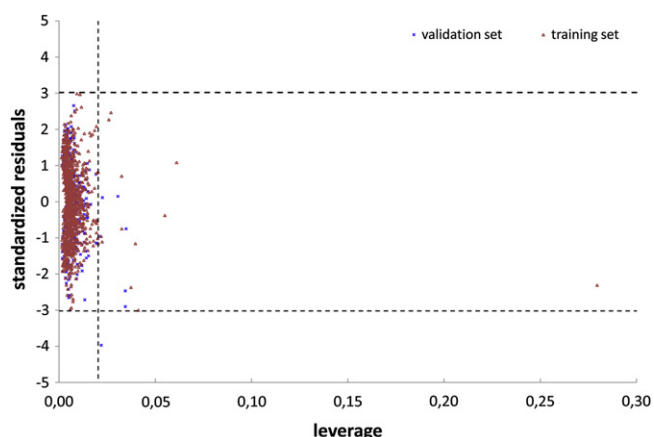
Fig. 3. Williams plot for the selected mtc-QSAR.

In order to obtain the multi-target QSAR models, it was necessary to calculate also molecular descriptors different among all the TKs. The corresponding values of the spectral moments for each TK were not directly calculated, because the MODES-LAB software was not able to calculate the molecular descriptors for so large molecular entities. Thus, we decided to calculate the spectral moments for each TK as the average values of the relative inhibitors active at the given cut-off of activity. For example, the dipole ($^d\mu$) spectral moments at the 4th calculation step for EGFR at 0.1 μM were:

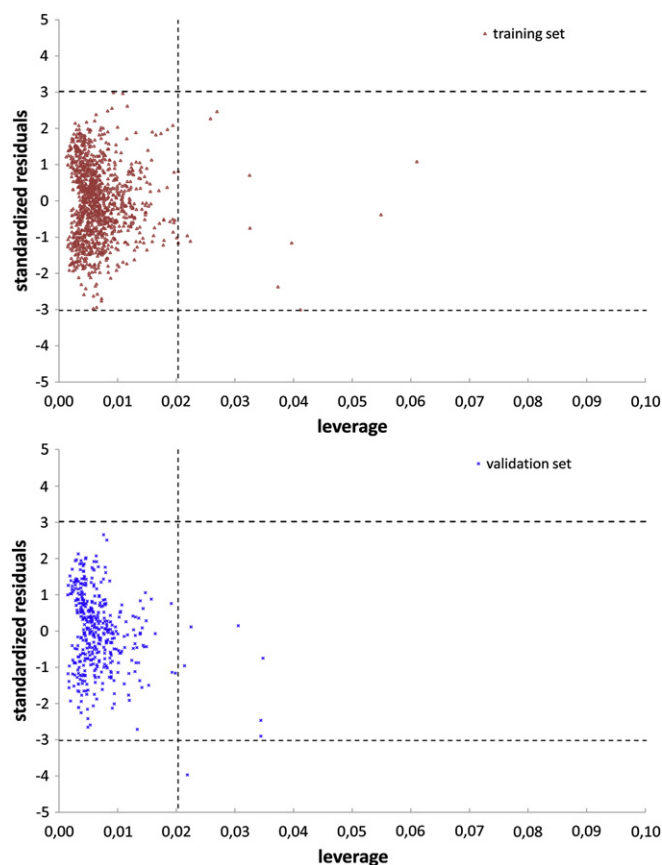$$\langle^d\mu\rangle_4(\text{EGFR})_{0.1} = \sum(^d\mu_{4,C=1})/n \qquad (1)$$

Fig. 4. Williams plots for the training set (top) and for the validation set (bottom) separately. Note that the graphics have been truncated at leverage = 0.10 for clarity.

In which: $^d\mu_{4,C=1}$ states for the values of the dipole moments at the 4th calculation step for those n compounds tested against EGFR and active ($C = 1$) at 0.1 μM. Finally, to each m case was associated another set of descriptors, $\Delta(^{weight}\mu_{k,i})$, calculated as the difference between the corresponding descriptors for the compound i and the average spectral moment associated to the TKs. For example, for the case $m = 500$ (which was a compound assayed against EGFR), the dipole moment at the 4th calculation step and with a cut-off of activity of 0.1 μM was:

$$\Delta(^d\mu_{4,500})_{0.1} = {}^d\mu_{4,500} - \langle^d\mu_4\rangle(\text{EGFR})_{0.1} \qquad (2)$$

On the whole, three classes of molecular descriptors have been thus considered to derive the models, for a total amount of 135 independent variables:

1. a series of compound related spectral moments (generally indicated as $^{weight}\mu_{k,i}$). Because of the values were directly calculated from the structures of the TKI, the molecular descriptors resulted as a characteristic of each i compound;
2. a series of target related spectral moments (generally indicated as $<^{weight}\mu_k>(TK)_{,\text{cut-off}}$). The values depended from both the TK and the cut-off of activity;
3. a series of case related spectral moments (generally indicated as $\Delta(^{weight}\mu_{k,m})_{\text{cut-off}}$). The values depended from the TK, the TKI and the cut-off of activity.

Each series of spectral moments contained 45 descriptors (9 bond weight types per 5 calculation steps). All the variable values have been standardized, in order to obtain a more rigorous statistical analysis.

The mtc-QSAR models were derived using the Linear Discriminating Analysis (LDA) module of the STASTICA 6.0 software package [20]. For each cut-off of activity the subset variable selection was performed employing the *forward stepwise* algorithm. The number of steps was adjusted so that at least one molecular descriptor associated to the TK entered the model. The statistical significance of the LDA models was determined calculating the p-level (p) of error with F-test and the Chi-squared test. Specificity, Sensitivity, and total Accuracy were also determined to assess the quality-of-fit to data in training. Finally the domain of applicability of the QSAR models was assessed as previously described [21].

3. Results and discussion

3.1. QSAR models generation

In order to develop several multi-target classification QSAR models useful to assess the activity profile of the TKIs, the literature data regarding the 2D structure and the IC_{50} (or the pIC_{50}) values of several compounds were collected. All the compounds included in the dataset had been assayed against at least one of a set of TKs involved in the cancer disease. In particular, the TKs considered in this work could be divided in cytoplasmic TKs (abl, lck and src) and in receptor TKs (EGFR, FGFR1, KDR, PDGFRβ and VEGFR-1). Moreover, in order to eliminate errors arising from the use of different measurement protocols, the only TKIs whose inhibitory activity was tested on a synthetic poly-Tyr peptide were introduced into the dataset. By this way, 1300 different TKIs were collected, for a total amount of 1771 cases as several compounds were assayed versus several TKs. Statistics regarding the employed dataset are reported in Table 3.

TKIs revealed a high degree of structural variability (Fig. 1), and presented a broad activity range (from 3 pM to up than 100 μM).
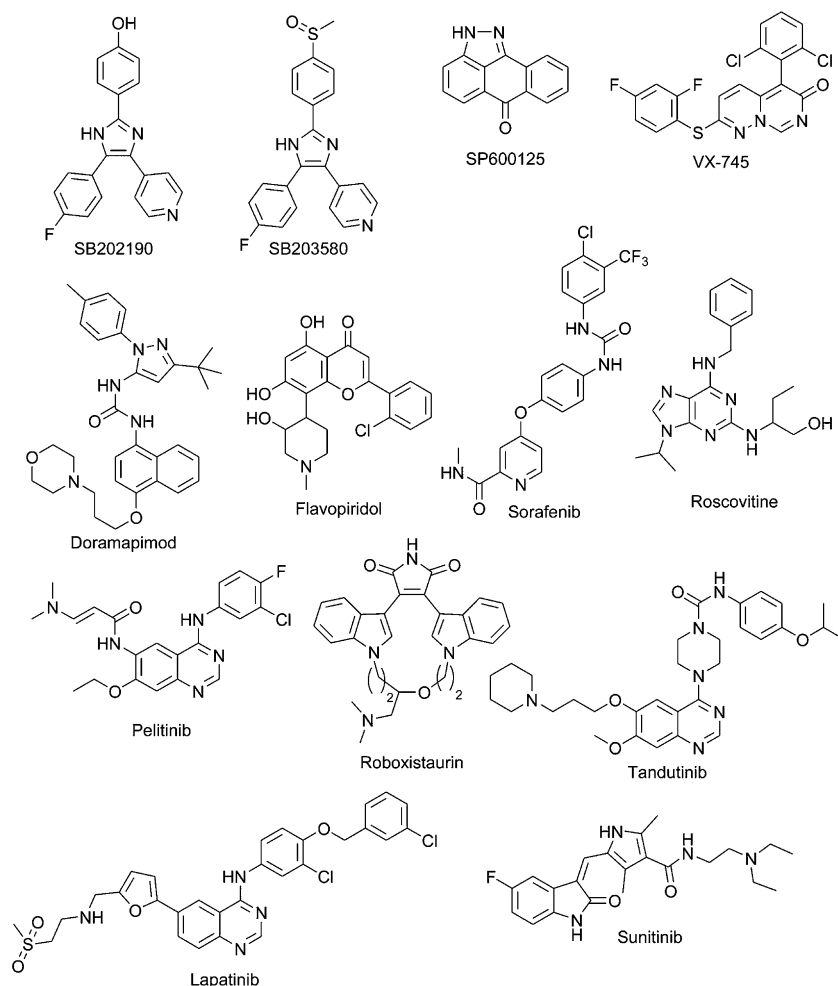
Fig. 5. Previously reported compounds selected for external validation.

To generate the 5 mtc-QSAR models, 5 cut-off of activity were considered (see Table 4 for values). The employment of 3D structural derived molecular descriptors has been hedged; in fact, the 3D approaches require computationally expensive optimization algorithms and start from the often incorrect assumption that the minimum energy conformation overlap the best geometry for drug–target interaction. Moreover the interaction geometries of such non homogenous set of cases have to be highly different and, even if the sequence of all considered TKs has been reported, not the same is for the 3D structures. For the TKIs, a set of molecular descriptors have been directly calculated starting from the SMILES code, applying the TOPS-MODE approach of the MODES-LAB software. For the TKs descriptor determination, a different approach has been handled: each molecular descriptor associated to each TK was considered as the average value of those of all related TKIs active at the given cut-off. Moreover, another set of descriptors have been associated to each TK, calculated as the difference between the corresponding descriptors for the compound and the average spectral moment associated to the TKs (see Material and Methods for a more detailed description). The overall dataset

Table 5
Predicted vs actual observed activity profile for the 13 known kinases inhibitors.

| Compound	Predicted class @ 0.1 μM							Observed class @ 0.1 μM						
	abl	lck	src	EGFR	FGFR1	KDR	PDGFRβ	abl	lck	src	EGFR	FGFR1	KDR	PDGFRβ
SB202190	0	0	0	0	0	0	0	0	0	0	0	0	0	0
SB203580	0	0	0	0	0	0	0	0	0	0	0	0	0	0
VX745	0	0	0	0	0	0	0	0	0	0	0	0	0	0
Doramapimod	0	0	0	0	0	0	0	0	0	0	0	0	0	0
SP600125	0	0	0	0	0	0	0	0	0	0	0	0	0	0
Lapatinib	0	1	1	1	1	1	0	0	0	0	1	0	0	0
Pelitinib	1	1	1	1	1	1	1	0	1	0	1	0	0	0
Sunitinib	0	0	0	0	0	0	0	0	0	0	0	0	1	1
Tandutinib	0	0	1	1	0	1	0	0	0	0	0	0	0	1
Roboxistaurin	0	0	0	0	0	0	0	0	0	0	0	0	0	0
Sorafenib	1	1	1	1	1	1	1	0	0	0	0	0	1	1
Roscovitine	0	0	1	1	0	1	0	0	0	0	0	0	0	0
Flavopiridol	0	0	0	0	0	0	0	0	0	0	0	0	0	0
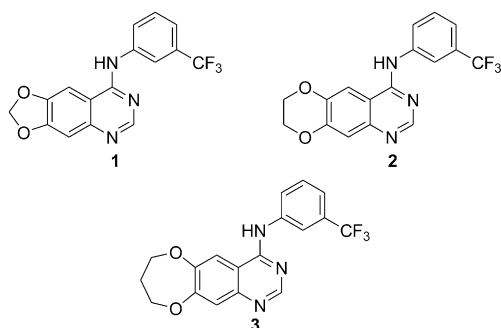
Fig. 6. Quinazoline derivatives used to evaluate the QSAR models.

have been randomly split into a *training set* (containing about the 75% of the cases) and an *internal validation set* (containing the remaining 25% of the cases). The purpose of the internal validation set was to assess in a more rigorous manner the internal pre-dictivity of the models. All the variables have been standardized and the mtc-QSAR models have been derived through linear discriminant analysis. The statistical significance and the quality of the QSAR models are reported in Table 4.

Based on the higher accuracy value and on the relative low number of false positive revealed, the mtc-QSAR model derived at a cut-off of 0.1 μM has been selected for further investigations. The selected model showed the below reported equation (coefficients are relative to standardized molecular descritpors).

$$\text{Score} = -0.99\,{}^{d}\mu_1 - 0.75\,{}^{h}\mu_1 + 3.97\,{}^{ps}\mu_1 + 1.99\,{}^{ps}\mu_5$$
$$+0.51\,{}^{m}\mu_2 - 7.01\,\Delta({}^{ps}\mu_2) - 4.49\,\Delta({}^{p}\mu_3)$$
$$+5.74\,\Delta({}^{m}\mu_1) - 0.59$$

In the reported equation, the first five molecular descriptors are compound related, while the last three are target related. When the score of a compound resulted >0.50, the compound was classified as active against the considered TK.

The ability to discriminate between active and inactive compounds with respect to each TK have been calculated (see Fig. 2 for a graphical representation of the results), as well as the domain of applicability (Figs. 3 and 4).

In order to assess the effectiveness in prediction, the selected models have been requested to classify a set of 13 known compounds (Fig. 5) for which the selective profile had been previously reported (Table 5). For all the compounds the IC$_{50}$ against 7 of the 8 TKs considered had been reported. Except for Lapatinib, Pelitinib, Tandutinib and Sorafenib the selectivity profile

Table 6
Predicted and observed classifications for compounds **1**–**3**.

Compound	Kinase	Predicted class @ 0.1 μM	Observed class @ 0.1 μM
1	abl	0	0
	EGFR	0	0
	FGFR-1	0	0
	KDR	0	0
	PDGFRβ	1	0
2	abl	0	0
	EGFR	0	0
	FGFR-1	0	0
	KDR	0	0
	PDGFRβ	1	1
3	abl	0	0
	EGFR	0	0
	FGFR-1	0	0
	KDR	0	0
	PDGFRβ	1	0

has been predicted in a satisfactory manner, with an overall accu-racy of 74.73%. For SB202190, SB203580, VX745, Doramapimod, SP600125, Roboxistaurin and Flavopiridol the model resulted in 100% accuracy, while for Sunitinib and Roscovitine the accuracies found were 74.40% and 57.10% respectively. Interestingly, the compounds for which the lower accuracy in prediction was found (Lapatinib, Pelitinib, Tandutinib and Sorafenib), belong to the so called "type II" class of TKIs [22]. Type II TKIs occupy a hydrophobic site that is directly adjacent to the ATP binding pocket. This addi-tional site characterizes the inactive conformation of the TKs. The amino acids surrounding this hydrophobic pocket are less conserved with respect to those in the ATP binding pocket and it has been proposed that the interaction with this accessory pocket leads to a higher selectivity profile. In the herein considered training set, a very low percentage of compounds (less than 5%) belong to the type II TKIs, and consequently the model resulted unable to correctly classify this kind of compounds. It appears thus reasonable that a specific model for the type II TKIs should be developed.

On the whole, except for the case of Roscovitine, the model resulted able to identify those compounds which resulted totally inactive against the panel of the considered TKs (SB202190, SB203580, VX745, Doramapimod, SP600125, Sunitinib, Robox-istaurin and Flavopiridol).

Finally, because of our interest in discovery of novel promising TKIs, we firstly predicted and then determined the biological profile of three quinazoline derivatives (Fig. 6), which have been previ-ously synthesized by our research group [14].

The model resulted able to predict in a satisfactory manner the activity profile for the titled compounds (Table 6). It is noteworthy that all the three compounds have been predicted able to inhibit PDGFRβ at 0.1 μM, whilst only compound **2** resulted as active from the biological evaluation. However, compounds **1** and **3** were not totally inactive against the enzyme: both compounds resulted in about 40% inhibition at the considered concentration. Thus, the prediction of the model has not to be considered as totally wrong.

4. Conclusions

In this work, 5 multi-target QSAR models for TKIs classification have been developed. All the models have been derived through a linear discriminant analysis and resulted in overall accuracy higher than 80%. In all the cases, the models have been constructed starting from a set of 1300 literature reported compounds and have been validated through an internal validation set. All the models have been developed using TOPS-MODE based molecular descrip-tors associated to the TKIs. The same descriptors have been employed to mathematically derive several TKs associated descriptors. The best model has been submitted to further valida-tions, using both an external set of previously reported TKIs and three novel compounds. Because of the good accuracy of the model, it could represent an useful tool to find novel promising kinases inhibitors. Moreover, since the model takes in consideration a set of 8 different enzymes, it could be employed to search for novel TKIs with specific activity profile in virtual screening processes.

Appendix. Supplementary data

Supplementary data associated with this article can be found in the online version, at doi:10.1016/j.ejmech.2011.02.072.

References

[1] J. Dancey, E.A. Sausville, Nat Rev Drug Discov 2 (2003) 296.
[2] P. Cohen, Nat Rev Drug Discov 1 (2002) 309.
[3] J. Mendelsohn, J Clin Oncol 20 (2002) 1S.
[4] M. Krug, A. Hilgeroth, Mini Rev Med Chem 8 (2008) 1312.
[5] A. Petrelli, S. Giordano, Curr Med Chem 15 (2008) 422.
[6] A.R. Dluzewski, C.R. Garcia, Experientia 52 (1996) 621.
[7] G. Gargala, A. Baishanbo, L. Favennec, A. Francois, J.J. Ballet, J.F. Rossignol, Antimicrob Agents Chemother 49 (2005) 4628.
[8] I. Kufareva, R. Abagyan, J Med Chem 51 (2008) 7921.
[9] M.H. Potashman, J. Bready, A. Coxon, T.M. DeMelfi Jr., L. DiPietro, N. Doerr, D. Elbaum, J. Estrada, P. Gallant, J. Germain, Y. Gu, J.C. Harmange, S.A. Kaufman, R. Kendall, J.L. Kim, G.N. Kumar, A.M. Long, S. Neervannan, V.F. Patel, A. Polverino, P. Rose, S. Plas, D. Whittington, R. Zanon, H. Zhao, J Med Chem 50 (2007) 4351.
[10] F.A. Pasha, M. Muddassar, A.K. Srivastava, S.J. Cho. J Mol Model, 16, 263.
[11] L.L. Zhu, T.J. Hou, L.R. Chen, X.J. Xu, J Chem Inf Comput Sci 41 (2001) 1032.
[12] W.M. Shi, Q. Shen, W. Kong, B.X. Ye, Eur J Med Chem 42 (2007) 81.
[13] X.H. Ma, R. Wang, C.Y. Tan, Y.Y. Jiang, T. Lu, H.B. Rao, X.Y. Li, M.L. Go, B.C. Low, Y.Z. Chen. Mol Pharm.
[14] A. Chilin, M.T. Conconi, G. Marzaro, A. Guiotto, L. Urbani, F. Tonus, P. Parnigotto, J Med Chem 53 (2010) 1862.
[15] Chemaxon Marvin 5.3 Program, Budapest, Hungary. www.chemaxon.com/products.htm
[16] E. Estrada, S. Vilar, E. Uriarte, Y. Gutierrez, J Chem Inf Comput Sci 42 (2002) 1194.
[17] E. Estrada, A. Pena, R. Garcia-Domenech, J Comput Aided Mol Des 12 (1998) 583.
[18] E. Estrada, J Chem Inform Comput Sci 36 (1996) 844.
[19] E. Estrada, E. Molina, J Mol Graph Model 20 (2001) 54.
[20] StatSoft. Inc., 6.0 ed., 2002.
[21] P. Gramatica, Qsar Comb Sci 26 (2007) 694.
[22] Y. Liu, N.S. Gray, Nat Chem Biol 2 (2006) 358.